

# Role of Intramolecular Torsion and Solvent Dynamics in the Charge-Transfer Kinetics in Triphenylphosphine Oxide Derivatives and DMABN

Pascale Changuenet, Pascal Plaza, Monique M. Martin,\* and Yves H. Meyer

Laboratoire de Photophysique Moléculaire du CNRS (UPR 3361), Bâtiment 213,  
Université Paris-Sud, 91405 Orsay, France

Received: May 30, 1997; In Final Form: July 24, 1997<sup>⊗</sup>

The photoinduced processes in three dimethylamino derivatives of the triphenylphosphine oxide (OMAP, ODAP, and OTAP) are studied in solution at room temperature by time-resolved fluorescence spectroscopy with a streak camera and a 500 fs UV laser excitation source. These compounds exhibit a dual fluorescence in polar solvents explained by the fast formation of an emissive charge-transfer state as in the model compound (dimethylamino)benzonitrile (DMABN). Fluorescence decays are also measured for solutions of DMABN under the same conditions. For both compounds, the intramolecular charge-transfer time is shown to vary from a few picoseconds to a few tens of picoseconds depending on the polarity of the solvent and, for the triphenylphosphine derivatives, on the number of dimethylamino substituents. The charge-transfer process is described as a barrier-activated process with a solvent polarity dependent height. The solvent dynamics and solvent viscosity effects on the charge-transfer rate are examined for both the (dimethylaminophenyl)diphenylphosphine oxide (OMAP) and DMABN. In protic solvents, the charge-transfer time is found to be shorter than the average solvation time for both compounds, suggesting that the charge-transfer mechanism involves an intramolecular coordinate in addition to the solvent coordinate. The charge-transfer times found for DMABN are in good agreement with those recently calculated by Kim and Hynes (*J. Photochem. Photobiol. A* 1997, 105, 337–343), who derived a two-dimensional model using the initially proposed twisting motion of the dimethylamino group as the intramolecular coordinate. The twisting motion of the whole aniline moiety is discussed as the possible intramolecular motion for OMAP on the basis of the solvent viscosity effects, which are found to differentiate this compound from DMABN.

## 1. Introduction

The excited-state processes in (dimethylamino)benzonitrile (DMABN, Figure 1, right) have given rise to a wide range of experimental<sup>1–20</sup> and theoretical studies.<sup>21–24</sup> To explain the dual fluorescence of this compound in polar solvents, Grabowski et al. proposed a reaction scheme involving intramolecular charge transfer with a 90° twisting motion of the dimethylamino group, leading to the formation of an emissive transient species called the TICT state.<sup>1–3</sup> Time-resolved fluorescence<sup>6–13,16,19</sup> and transient absorption<sup>15,25</sup> measurements brought support to the proposal of a photoinduced charge-transfer process in DMABN, but it comes out that the structural change is not well characterized yet and still disputed. Studies of bridged derivatives led the authors to conclude that the dual fluorescence requires the free rotation of the dimethylamino group<sup>2,3</sup> but recently a pyramidalization motion was suggested.<sup>19,20</sup> On the other hand, the observation of a transient absorption spectrum similar to that of the benzonitrile radical anion gave support to a mechanism involving the orbital decoupling of the donor and acceptor moieties in the excited state.<sup>15</sup>

The concept of photoinduced charge transfer involving a geometrical change has been extended to a wide variety of flexible compounds containing electron donor and acceptor groups.<sup>26,27</sup> The triphenylphosphines are propeller-type compounds with a pyramidal geometry. Their dimethylamino derivatives (MAP, DAP, TAP, Figure 1, left) were reported to exhibit a dual fluorescence in polar solvents.<sup>28–30</sup> Recent studies gave evidence that the solvent-dependent dual fluorescence is due to the oxidized form of these derivatives (for example, OMAP in Figure 2).<sup>31,32</sup> Trivalent phosphorus is sensitive to

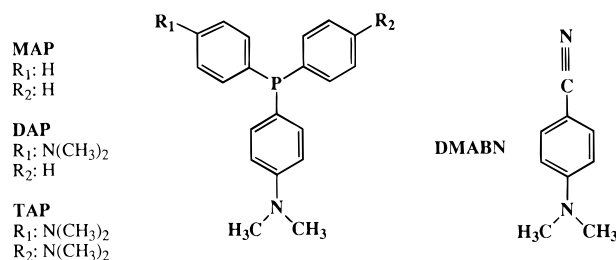


Figure 1. Dimethylamino derivatives of triphenylphosphine (MAP, DAP, TAP) and (dimethylamino)benzonitrile (DMABN).

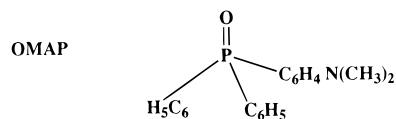


Figure 2. (Dimethylaminophenyl)diphenylphosphine oxide (OMAP).

oxygen, and its oxidized form is very stable. Oxidation of the phosphorus atom in (dimethylamino)triphenylphosphine derivatives was shown to occur during or after preparation of solutions<sup>31,32</sup> depending on the solvent, the solute concentration, and how long the solutions were exposed to air. In tetrahydrofuran, where the phosphines are easily oxidized due to the presence of peroxides, time-resolved fluorescence measurements gave evidence for a precursor-successor relationship between the two fluorescence bands.<sup>29–31</sup> From the solvatochromism of the red-edge band in solvents of increasing polarity, a dipole moment of about 20 D was deduced<sup>31</sup> for the transient emissive state by using Weller's equation.<sup>33</sup> On the other hand, a transient absorption band with a profile similar to that of the dimethylaniline cation radical was observed in this solvent,<sup>29–31</sup> showing that the charge transfer takes place from the dimeth-

<sup>⊗</sup> Abstract published in *Advance ACS Abstracts*, October 1, 1997.

ylaniline donor group in agreement with the initial Vogel et al. proposal.<sup>28</sup> However, since in these compounds the dimethylaniline group is not much coupled to the remaining part of the molecule (Figure 2), one cannot tell whether the charge-transfer reaction is accompanied by the rotational motion of the donor part or not. In the present study, we measured the charge-transfer time in the triphenylphosphine oxide derivatives in a series of polar solvents at room temperature by time-resolved fluorescence spectroscopy. Fluorescence decay measurements were also carried out for the model compound DMABN under the same conditions since very few data were available at room temperature. The role of an intramolecular twisting motion in the charge-transfer process is discussed for both compounds.

## 2. Experimental Section

**2.1. Subpicosecond Laser Source.** The subpicosecond laser system used for these experiments is a non mode-locked, homemade, dye-laser system.<sup>34</sup> The system produces 500 fs, 400  $\mu$ J pulses at 610 nm starting from a single seeded Q-switched Nd:YAG laser (6 ns, 10 Hz). High-power tunable pulses in the 400–800 nm wavelength range can be produced by focusing the 610 nm pulses in a 2 cm water cell to generate a continuum of white light, filtering the continuum at the desired wavelength and amplifying the filtered beam in dye amplifiers pumped by either the second or the third harmonic of the Nd:YAG laser. For the present study, the laser system was tuned at 570 nm and a subpicosecond excitation source at 285 nm was provided by frequency-doubling the 500 fs pulses of the fundamental beam.

**2.2. Time-Resolved Fluorescence Measurements.** The samples were excited with 5–10  $\mu$ J of the subpicosecond pulses at 285 nm, and the fluorescence decays were recorded with a 4 ps time-response streak camera (ARP, Strasbourg, France). The fluorescence was collected at the magic angle. Since the samples exhibit dual fluorescence, the decay of each fluorescence band was measured separately, with a Schott UG11 filter for the short-wavelength edge of the spectrum and a set of different "wratten" Kodak filters for the long-wavelength edge. A properly advanced reference pulse of the fundamental beam at 570 nm and the fluorescence decay were recorded on the same camera trace. An average decay trace over 500–1000 shots was obtained by superposition of the reference pulse of each trace to eliminate the jitter in triggering the camera sweep. The fluorescence decays were fitted with exponential functions reconvoluted with the response function of the camera.<sup>31</sup> When needed the preexponential factors were corrected<sup>31</sup> from the overlap of the two fluorescence bands, the transmission spectrum of the filter plus the entrance optics of the camera, and the response of the photocathode (S20).

**2.3. Compounds.** The (dimethylaminophenyl)diphenylphosphine (MAP), bis(dimethylaminophenyl)phenylphosphine (DAP), and tri(dimethylaminophenyl)phosphine (TAP) (Figure 1, left) were provided by W. Rettig from the Humboldt University, but part of the experiments were done with the (dimethylaminophenyl)diphenylphosphine (MAP) purchased from Aldrich and used without further purification. The (dimethylamino)-benzonitrile (DMABN, Figure 1, right) was purchased from Fluka and purified by several sublimations and recrystallizations according to the method advised by F. Heisel.<sup>9–12</sup> All solvents were UV-spectroscopy grade (Merck), except decanol (Jansen) and triacetin (Aldrich) for which the absence of fluorescent impurities was checked with the streak camera. The phosphine samples were prepared under atmospheric conditions and kept in the dark at room temperature until the substituted phosphines were fully oxidized (Figure 2).<sup>31,32</sup> The presence of the oxidized

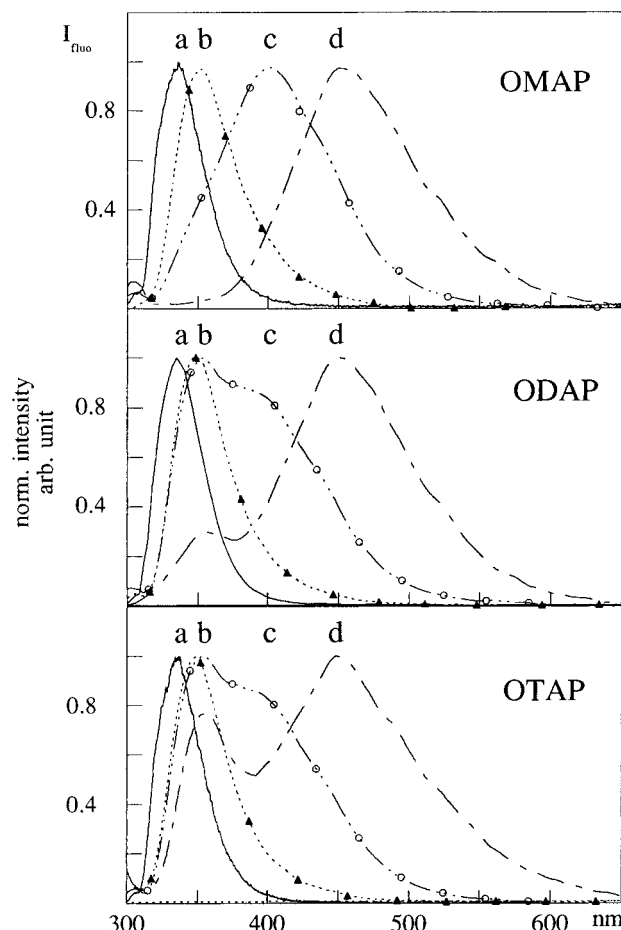


**Figure 3.** Normalized fluorescence spectra of the dimethylamino-substituted triphenylphosphine oxides (OMAP, ODAP, OTAP) in solvents of increasing polarity: cyclohexane (a), dioxane (b), tetrahydrofuran (c), and acetonitrile (d).

form in the solution was checked by inspection of the absorption spectra. The spectrum of the dimethylamino derivatives of the triphenylphosphine oxide is narrower and slightly blue-shifted from that of the nonoxidized form; the shoulder around 260 nm is lacking but a new small shoulder can be seen around 225 nm.<sup>35</sup> For the time-resolved fluorescence experiments, the concentration was chosen so that the excitation light at 285 nm was totally absorbed in a 1 mm cell. The solutions were recirculated and deaerated with a nitrogen flow during the measurements.

## 3. Results

**3.1. Steady-State Dual Fluorescence.** The steady-state fluorescence spectra of solutions containing the oxidized form of the dimethylamino-substituted triphenylphosphines in solvents of increasing polarity<sup>30–32</sup> are shown in Figure 3. Those observed for DMABN are given in Figure 4. In all cases, the spectra can be decomposed into two subbands, one of them exhibiting a large solvatochromism. The blue-edge band is attributed to the locally excited (LE) state and the red-edge one to the charge-transfer (CT) state. In the case of DMABN, the latter is the well-known TICT state.<sup>1–4</sup>

**3.2. Time-Resolved Fluorescence.** (a) *Fluorescence Decays in Fluid Aprotic Solvents.* The fluorescence decays of OMAP and DMABN in a series of aprotic solvents of increasing polarity were both measured in the wavelength ranges below 400 nm and above 450 nm. The solvents are listed in Table 1 (upper part). Their viscosity is  $\leq 1.5$  cP and their average solvation time  $\leq 2.6$  ps. In the weakly and strongly polar solvents, the

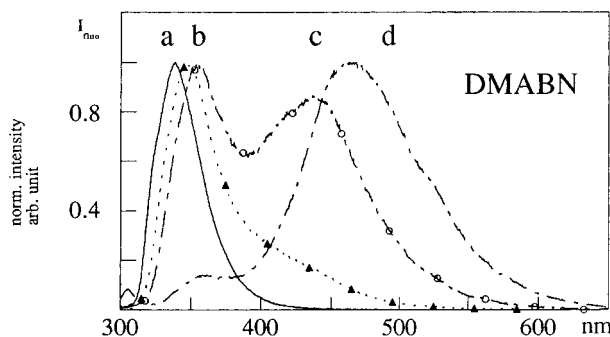


**Figure 4.** Normalized fluorescence spectra of DMABN in solvents of increasing polarity: cyclohexane (a), diethyl ether (b), tetrahydrofuran (c), and acetonitrile (d).

**TABLE 1: Dielectric Constant, Viscosity, and Average Solvation Time of the Aprotic Solvents Used in the Present Study<sup>a</sup>**

solvent	$\epsilon^{58}$	$\eta$ (cP) <sup>58</sup>	$\langle\tau_s\rangle$ (ps) <sup>36</sup>
cyclohexane	2.02 (20 °C)	0.98 (20 °C)	1.7
dioxane	2.21 (25 °C)	1.44 (15 °C)	
diethyl ether	4.33 (20 °C)	0.24 (30 °C)	2.6 <sup>59</sup>
ethyl acetate	6.02 (25 °C)	0.43 (25 °C)	
tetrahydrofuran	7.58 (25 °C)	0.55 (20 °C)	0.94
acetonitrile	37.50 (20 °C)	0.37 (30 °C)	0.26
triacetin	7.11 (20 °C) <sup>60</sup>	22 (20 °C) <sup>60</sup>	125 <sup>61</sup>

<sup>a</sup> In the upper part, the fluid solvents are listed by increasing polarity. In the lower part, triacetin is the solvent used to test solvent viscosity effect at constant polarity by comparison with tetrahydrofuran.

time-resolved fluorescence intensity could be fitted with a two-exponential function, with a picosecond decay followed by a nanosecond decay for  $\lambda < 400$  nm and a picosecond rise followed by a nanosecond decay for  $\lambda > 450$  nm. The time components ( $\tau_i$ ) and preexponential factors ( $c_i$  for  $\lambda < 400$  nm and  $c'_i$  for  $\lambda > 450$  nm) are given in Table 2 for OMAP and Table 3 for DMABN. For example, the decays observed for OMAP in tetrahydrofuran are given in Figure 5, and those observed for DMABN in acetonitrile are given in Figure 6. The selected spectral ranges were chosen in order to try to follow the population kinetics of the LE state ( $<400$  nm) and CT state ( $>450$  nm) separately. However, in the wavelength range below 400 nm, the LE state and CT state fluorescence bands partly overlap. In weakly polar solvents, the overlap may be large in the observation window as shown in Figure 7 for OMAP in tetrahydrofuran. Therefore the preexponential factors ( $c_1$  and  $c_2$ ) of the LE state decay-components were corrected;<sup>31</sup> the corrected values ( $b_1$  and  $b_2$ ) are indicated within brackets in Tables 2 and 3. It is interesting to note that in all solvents, the initial picosecond decay component of the LE state is found to be equal to the rise component of the CT state. Furthermore, this initial time component is found to decrease when the solvent polarity increases. It is also found to be shorter in OMAP than in DMABN, in polar solvents.

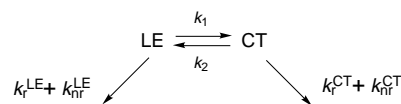
The fluorescence decay components and preexponential factors found for the LE state of the oxides of the three dimethylamino triphenylphosphine derivatives, OMAP, ODAP, and OTAP (Figure 1, left) in tetrahydrofuran, are compared in Table 4. It is seen that the initial decay component is slowed down when the number of dimethylamino substituents increases. Table 2 shows that the initial decay time of the LE state of OMAP becomes less than 3 ps in acetonitrile. For ODAP and OTAP in acetonitrile this initial decay time becomes, respectively, 6 and 9 ps, which confirms the increase of the short lifetime component with the number of dimethylamino substituents and its decrease when the solvent polarity increases.

(b) *Fluorescence Decays in Protic Solvents.* The protic solvents used are listed in Table 5 by increasing polarity. Their viscosity is less than 2 cP except for decanol and ethylene glycol, which are viscous with a viscosity of about 14 cP. In these solvents, the solvation times range from a few picoseconds to a few hundreds of picoseconds.<sup>36</sup> Therefore, the spectral shift of the charge-transfer state fluorescence due to the solvation dynamics is expected to occur within our observation time window, and the fluorescence decays were measured in three spectral ranges ( $\lambda < 400$  nm,  $\lambda > 450$  nm, and  $\lambda > 550$  nm). All decays were fitted with a two-exponential function. For example, Figure 8 shows the fits obtained for OMAP in ethanol and Figure 9 those obtained for DMABN in ethylene glycol. The time components of the LE state and CT state decays measured in the series of protic solvents are given in Table 6 for OMAP and in Table 7 for DMABN. It is seen that in both cases, the weight ( $c_2$ ) of the long component of the LE state is less than 3%, indicating that the decays are dominated by the fast initial component. Therefore correction of the preexponential factors by taking into account the remaining contribution of the CT state fluorescence in this wavelength range was not made. Tables 6 and 7 show that the LE state decay time of both compounds decreases when the solvent polarity increases, except for DMABN in ethylene glycol. The decay time remains shorter in OMAP than in DMABN, except in propanol. An other interesting point is that the decay time is found to be shorter than the solvation time, except for DMABN in methanol.

(c) *Solvent Viscosity Effect.* By comparing the charge-transfer kinetics in OMAP and in DMABN in aprotic solvents, when the solvent is changed from the fluid tetrahydrofuran to the viscous triacetin with roughly the same dielectric constant (Table 1, lower part), we found that the initial decay of the LE state of OMAP is slowed by a factor of 6 whereas that of DMABN is slowed down by a factor of 1.5 only (Tables 2 and 3, lower part). The viscosity of triacetin is 40 times larger than that of tetrahydrofuran. Their average solvation times are also much different, and in triacetin the charge transfer kinetics becomes faster than the solvation dynamics for both compounds. A much larger decrease of the rate is found for both compounds when the solvent is changed from tetrahydrofuran to the protic solvent decanol, which has the same polarity but is 1.6 times less viscous than triacetin (Table 5). The decrease is roughly a factor 13 for OMAP and 8 for DMABN (Tables 6 and 7).

## 4. Discussion

**4.1. Charge-Transfer Reaction Scheme.** (a) *Aprotic Solvents.* Tables 2 and 3 show that in both OMAP and DMABN, the initial decay component of the LE state is equal to the rise component of the CT state. This observation gives evidence to a precursor–successor relationship between the two states. On the other hand, the LE and CT states are found to have the same long-component decay, fairly well separated from the initial fast component, which shows that their population ratio reaches equilibrium during the excited-state lifetime. The reaction scheme shown below, which was initially proposed for DMABN,<sup>2</sup> can thus be applied to OMAP:



Considering this scheme, the time-resolved fluorescence intensity of the LE and CT states can be described by the following set of equations

**TABLE 2: Time Components ( $\tau_i$ ) and Preexponential Factors ( $c_i$  and  $c'_i$ ) Obtained from the Fit of the Time-Resolved Fluorescence Intensities of OMAP Solutions in the Aprotic Solvents Listed in Table 1<sup>a</sup>**

OMAP/solvent	$\tau_{LE}$ $\lambda < 400$ nm	$c_1 (b_1)$ $c_2 (b_2)$	$\Delta G_{LE \rightarrow CT}$ kcal/mol	$\tau_{CT}$ $\lambda > 450$ nm	$c'_1$ $c'_2$
cyclohexane	1.9 $\pm$ 0.1 ns	1			
dioxane	16 $\pm$ 2 ps	0.39 (0.54)	-0.1	16 $\pm$ 2 ps	-0.49
	1.1 $\pm$ 0.1 ns	0.61 (0.46)		1.2 $\pm$ 0.1 ns	0.51
diethyl ether	13 $\pm$ 2 ps	0.30 (0.48)	+0.05	15 $\pm$ 2 ps	-0.49
	1.0 $\pm$ 0.1 ns	0.70 (0.52)		1.2 $\pm$ 0.1 ns	0.51
ethyl acetate	11 $\pm$ 1 ps	0.79 (0.90)	-1.3	11 $\pm$ 1 ps	-0.50
	1.3 $\pm$ 0.1 ns	0.21 (0.10)		1.5 $\pm$ 0.1 ns	0.50
tetrahydrofuran	7 $\pm$ 1 ps	0.84 (0.95)	-1.8	7 $\pm$ 1 ps	-0.48
	1.2 $\pm$ 0.1 ns	0.16 (0.05)		1.3 $\pm$ 0.1 ns	0.52
acetonitrile	<3 $\pm$ 1 ps	0.97 (0.99)	<-2.8		
	3.2 $\pm$ 0.5 ns	0.03 (<0.01)		3.7 $\pm$ 0.1 ns	1
triacetin	40 $\pm$ 10 ps	0.83		37 $\pm$ 10 ps	-0.4
	2.1 $\pm$ 0.1 ns	0.17		2.4 $\pm$ 0.1 ns	0.6

<sup>a</sup> The wavelength ranges, respectively, below 400 nm and above 450 nm were chosen in order to follow the population kinetics of the LE state and CT state separately. Due to the overlap of the fluorescence bands of the two states below 400 nm, the preexponential factors ( $c_1$  and  $c_2$ ) of the LE state decay components were corrected;<sup>31</sup> the corrected values ( $b_1$  and  $b_2$ ) are indicated within brackets.

**TABLE 3: Time Components ( $\tau_i$ ) and Preexponential Factors ( $c_i$  and  $c'_i$ ) Obtained from the Fit of the Time-Resolved Fluorescence Intensities of DMABN Solutions in the Aprotic Solvents Listed in Table 1<sup>a</sup>**

DMABN/ solvent	$\tau_{LE}$ $\lambda < 400$ nm	$c_1 (b_1)$ $c_2 (b_2)$	$\Delta G_{LE \rightarrow CT}$ kcal/mol	$\tau_{TICT}$ $\lambda > 450$ nm	$c'_1$ $c'_2$
cyclohexane	2.8 $\pm$ 0.1 ns	1			
dioxan	24 $\pm$ 2 ps	0.68	-0.045	23 $\pm$ 2 ps	-0.48
	3.4 $\pm$ 0.1 ns	0.32		3.4 $\pm$ 0.1 ns	0.52
tetrahydrofuran	17 $\pm$ 1 ps	0.85 (0.88)	-1.2	17 $\pm$ 1 ps	-0.51
	3.9 $\pm$ 0.1 ns	0.15 (0.12)		3.9 $\pm$ 0.1 ns	0.49
acetonitrile	6 $\pm$ 1 ps	0.98 (0.99)	-2.8	6 $\pm$ 1 ps	-0.48
	2.9 $\pm$ 0.5 ns	0.02 (0.01)		2.9 $\pm$ 0.1 ns	0.52
triacetin	26 $\pm$ 1 ps	0.91		25 $\pm$ 1 ps	-0.49
	2.5 $\pm$ 0.5 ns	0.08		3.9 $\pm$ 0.1 ns	0.51

<sup>a</sup> The wavelength ranges, respectively, below 400 nm and above 450 nm were chosen in order to follow the population kinetics of the LE state and CT state separately. Due to the overlap of the fluorescence bands of the LE and CT state below 400 nm, the preexponential factors ( $c_1$  and  $c_2$ ) of the LE state decay components were corrected;<sup>31</sup> the corrected values ( $b_1$  and  $b_2$ ) are indicated within brackets.

$$i_{LE} = k_r^{LE} (b_1 e^{-\lambda_1 t} + b_2 e^{-\lambda_2 t}) \quad (1)$$

$$i_{CT} = k_r^{CT} \frac{k_1}{\lambda_1 - \lambda_2} [LE]_0 [e^{-\lambda_2 t} - e^{-\lambda_1 t}] \quad (2)$$

with

$$b_1 = \frac{1}{\lambda_1 - \lambda_2} (X - \lambda_2) [LE]_0 \quad (3)$$

$$b_2 = \frac{1}{\lambda_1 - \lambda_2} (\lambda_1 - X) [LE]_0 \quad (4)$$

$$X = k_1 + k_r^{LE} + k_{nr}^{LE} \quad Y = k_2 + k_r^{CT} + k_{nr}^{CT} \quad (5)$$

$$\lambda_{1,2} = \frac{(X + Y) \pm \{(X - Y)^2 + 4k_1 k_2\}^{1/2}}{2} \quad (6)$$

where  $k_1$  and  $k_2$  are respectively, the forward and backward reaction rate constants,  $k_r$  and  $k_{nr}$  the radiative and nonradiative decay rate constants, and  $[LE]_0$  is the initial concentration of the locally excited state produced by the excitation laser pulse. The initial concentration of the CT state is assumed to be  $[CT]_0 = 0$ . In Tables 2 and 3, it is seen that the preexponential factors of the rise and decay components of the CT state ( $c'_1$  with a negative sign and  $c'_2$ ) are found to be equal or close to each other, which is a good indication of the validity of the model since at time zero  $[CT]_0 = c'_1 + c'_2 = 0$ . The fact that the reaction reaches rapidly equilibrium indicates that  $k_1$  and  $k_2$  are

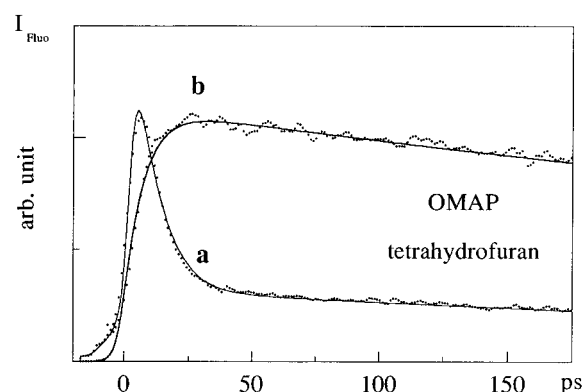


**Figure 5.** Normalized fluorescence decays measured for OMAP in tetrahydrofuran (streak speed 50 ps/mm), respectively below 400 nm (a) and above 450 nm (b), after excitation with a subpicosecond laser pulse at 285 nm. The time-resolved fluorescence intensities were fitted with a two-exponential function reconvoluted with the response function of the streak camera.

much larger than all the other rate constants. From the above set of equations, it can be easily shown that in such a case, one obtains

$$\lambda_1 = k_1 + k_2 \quad \text{and} \quad b_1/b_2 = k_1/k_2 \quad (7)$$

In Table 2 it is seen that for the polar solvents  $b_1 \gg b_2$  and thus  $k_1 \gg k_2$ . The charge-transfer time is thus directly given by the short-time component decay of the LE state. In dioxane and ethyl acetate,  $b_1 \approx b_2$  and thus  $k_1 \approx k_2$  and the charge-

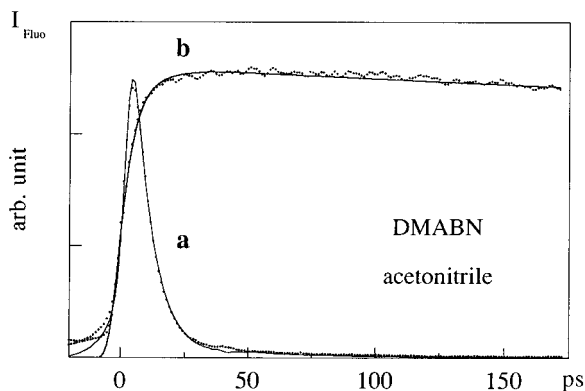


**Figure 6.** Normalized fluorescence decays measured for DMABN in acetonitrile (streak speed 50 ps/mm), respectively, below 400 nm (a) and above 450 nm (b), after excitation with a subpicosecond laser pulse at 285 nm. The time-resolved fluorescence intensities were fitted with a two-exponential function reconvoluted with the response function of the streak camera.

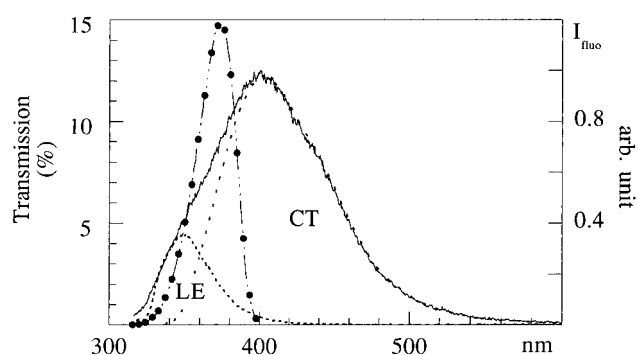


**Figure 7.** Steady-state fluorescence spectrum of OMAP in tetrahydrofuran (right scale) and transmission window of the detection ensemble (Schott UG11 filter plus streak camera entrance optics and photocathode response) when the wavelength range below 400 nm is selected (left scale).

**TABLE 4: Time Components ( $\tau_i$ ) and Corrected Preexponential Factors ( $b_i$ ) Obtained from the Fit of the Fluorescence Decay of the LE State of OMAP, ODAP, and OTAP in Tetrahydrofuran<sup>a</sup> ( $\lambda < 400$  nm)**

	OMAP	ODAP	OTAP
$\tau_{LE}(b_i)$	$7 \pm 1$ ps (0.95)	$11 \pm 2$ ps (0.90)	$16 \pm 2$ ps (0.80)
	$1.2 \pm 0.1$ ns (0.05)	$1.8 \pm 0.1$ ns (0.10)	$1.8 \pm 0.1$ ns (0.19)
$k_1$ (s <sup>-1</sup> )	$1.4 \times 10^{11}$	$8.2 \times 10^{10}$	$5.1 \times 10^{10}$
$k_2$ (s <sup>-1</sup> )	$9.8 \times 10^9$	$8.6 \times 10^9$	$1.2 \times 10^{10}$
$K = k_1/k_2$	20	9	4
$\Delta G_{LE-CT}$ (kcal·mol <sup>-1</sup> )	-1.8	-1.3	-0.83

<sup>a</sup> Rate constants of the forward ( $k_1$ ) and backward ( $k_2$ ) charge-transfer reaction, equilibrium constant  $K$ , and reaction free energy change  $\Delta G$  calculated for the three compounds from the measured kinetics.

transfer time is about twice the short-time component. Table 3 shows that the charge-transfer time in DMABN in polar solvents is also well described by the short-time component of the LE state decay. The 24 ps short component found for DMABN in dioxane is in good agreement with the value of 25 ps reported by Schuddeboom et al. for the CT state formation.<sup>19</sup> In acetonitrile, the reaction time is found to be 6 ps. The value was previously estimated to be less than 10 ps in fluorescence-decay measurements with lower time resolution.<sup>6</sup> A value of 4 ps was obtained from transient absorption measurements.<sup>25</sup>

(b) *Protic Solvents.* In protic solvents, the precursor-successor relationship between the LE and CT states does not

**TABLE 5: Dielectric Constant, Viscosity, and Average Solvation Time of the Protic Solvents Used in the Present Study<sup>a</sup>**

solvent	$\epsilon^{58}$	$\eta$ (cP) <sup>58</sup>	$\langle\tau_s\rangle$ (ps) <sup>36</sup>
1-decanol	7.9 (20 °C) <sup>62</sup>	14.3 (20 °C) <sup>62</sup>	245
2-propanol	19.92 (25 °C)	1.765 (30 °C)	
1-propanol	20.33 (25 °C)	1.722 (30 °C)	26
ethanol	24.55 (25 °C)	0.991 (30 °C)	16
methanol	32.70 (25 °C)	0.544 (25 °C)	5
ethylene glycol	37.70 (25 °C)	13.55 (30 °C)	15.3

<sup>a</sup> The fluid solvents are listed by increasing polarity.

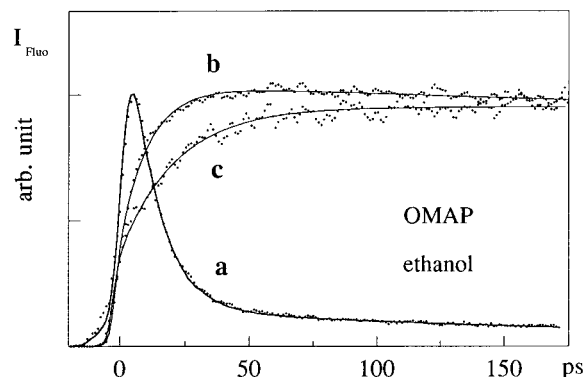


**Figure 8.** Normalized fluorescence decays measured for OMAP in ethanol (streak speed 50 ps/mm), respectively, below 400 nm (a), above 450 nm (b) and above 550 nm (c), after excitation with a subpicosecond laser pulse at 285 nm. The time-resolved fluorescence intensities were fitted with a two-exponential function reconvoluted with the response function of the streak camera.

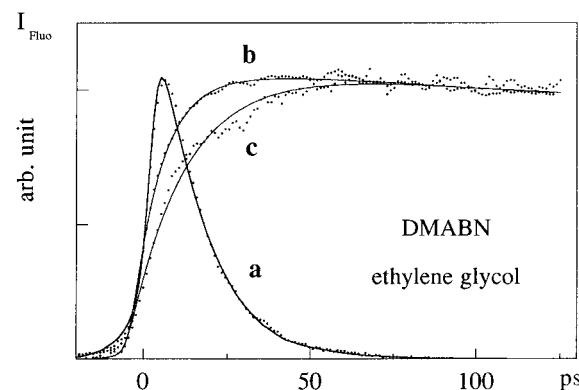


**Figure 9.** Normalized fluorescence decays measured for DMABN in ethylene glycol (streak speed 50 ps/mm), respectively below 400 nm (a), above 450 nm (b) and above 550 nm (c), after excitation with a subpicosecond laser pulse at 285 nm. The time-resolved fluorescence intensities were fitted with a two-exponential function reconvoluted with the response function of the streak camera.

appear clearly from the data given in Tables 6 and 7. This can be explained by the fact that a red-shift of the CT state fluorescence spectrum occurs as the result of the solvent reorganization around this highly polar species (at a rate given by the inverse of the average solvation time of Table 5), and the increase of the CT state population cannot be probed directly by following the CT state fluorescence rise time. It is indeed seen that the rise time is longer in the red-edge of the fluorescence band ( $\lambda > 550$  nm), for both OMAP and DMABN. This was previously reported for DMABN in protic solvents at low temperature by Heisel et al.<sup>12</sup> Thus, the same reaction scheme as in aprotic solvents can be used to describe the results of Tables 6 and 7, as long as the charge-transfer kinetics are deduced from the LE state decays. The fact that the weight ( $c_2$ ) of the long component of the LE state is weak (1–3%) indicates that the back reaction ( $k_2$ ) can be neglected and thus

**TABLE 6: Time Components ( $\tau_i$ ) and Preexponential Factors ( $c_i$  and  $c'_i$ ) Obtained from the Fit of the Time-Resolved Fluorescence Intensities of OMAP Solutions in the Protic Solvents Listed in Table 5<sup>a</sup>**

OMAP/ solvent	$\tau_{LE}(c_1)$	$\tau_{CT}(c'_1)$	$\tau_{CT}(c'_1)$
	$\tau_{LE}(c_2)$	$\tau_{CT}(c'_2)$	$\tau_{CT}(c'_2)$
	$\lambda < 400$ nm	$\lambda > 450$ nm	$\lambda > 550$ nm
1-decanol <sup>b</sup>	90 ± 10 ps (~1)	99 ± 10 ps (-0.40)	123 ± 10 ps (-0.4)
	2.0 ± 0.5 ns (<0.01)	2.8 ± 0.1 ns (0.60)	2.8 ± 0.1 ns (0.60)
2-propanol	25 ± 2 ps (0.98)	23 ± 2 ps (-0.49)	35 ± 2 ps (-0.50)
	3.0 ± 0.5 ns (0.02)	3.5 ± 0.1 ns (0.51)	3.5 ± 0.1 ns (0.50)
ethanol	10 ± 2 ps (0.97)	11 ± 1 ps (-0.45)	20 ± 1 ps (-0.41)
	2.9 ± 0.5 ns (0.03)	3.1 ± 0.1 ns (0.55)	3.1 ± 0.1 ns (0.58)
ethylene glycol	9 ± 1 ps (0.99)	12 ± 1 ps (-0.50)	16 ± 1 ps (-0.46)
	2.3 ± 0.5 ns (0.01)	3.3 ± 0.1 ns (0.50)	3.3 ± 0.1 ns (0.54)

<sup>a</sup> The wavelength ranges, respectively, below 400 nm and above 450 nm were chosen in order to follow the population kinetics of the LE state and CT state separately. <sup>b</sup> Rough experiment.

**TABLE 7: Time Components ( $\tau_i$ ) and Preexponential Factors ( $c_i$  and  $c'_i$ ) Obtained from the Fit of the Time-Resolved Fluorescence Intensities of DMABN Solutions in the Protic Solvents Listed in Table 5<sup>a</sup>**

DMABN/ solvent	$\tau_{LE}(c_1)$	$\tau_{CT}(c'_1)$	$\tau_{CT}(c'_1)$
	$\tau_{LE}(c_2)$	$\tau_{CT}(c'_2)$	$\tau_{CT}(c'_2)$
	$\lambda < 400$ nm	$\lambda > 450$ nm	$\lambda > 550$ nm
1-decanol <sup>b</sup>	140 ± 25 ps (~0.99)	200 ± 25 ps 3.3 ± 0.1 ns	
2-propanol	14 ± 1 ps (0.97)	21 ± 1 ps (-0.47)	36 ± 1 ps (-0.47)
	2.5 ± 0.5 ns (0.03)	3.0 ± 0.1 ns (0.53)	3.0 ± 0.1 ns (0.53)
ethanol	12 ± 1 ps (0.98)	10 ± 1 ps (-0.49)	18 ± 1 ps (-0.51)
	2.0 ± 0.5 ns (0.02)	2.3 ± 0.1 ns (0.51)	2.3 ± 0.1 ns (0.48)
methanol	8 ± 1 ps (0.99)	8 ± 1 ps (-0.40)	9 ± 1 ps (-0.47)
	1.6 ± 0.5 ns (0.01)	2.6 ± 0.1 ns (0.60)	2.6 ± 0.1 ns (0.53)
ethylene glycol	13 ± 1 ps (<0.9)	8 ± 1 ps (-0.49)	14 ± 1 ps (-0.50)
	1.0 ± 0.5 ns (>0.01)	1.3 ± 0.1 ns (0.51)	1.3 ± 0.1 ns (0.50)

<sup>a</sup> The wavelength ranges, respectively, below 400 nm and above 450 nm were chosen in order to follow the population kinetics of the LE state and CT state separately. <sup>b</sup> Rough experiment.

the charge-transfer time is directly given by the short time-decay component of the LE state in both compounds.

Several time-resolved fluorescence measurements were performed with DMABN, and the results are quite different. Multiexponential decays were observed in various alcohols at low temperature between -115 and -50 °C.<sup>9,10</sup> For temperatures between -50 and 0 °C, multiexponential decays were found in long chain alcohols whereas the short-time behavior of the decay could be accounted for by a single-exponential decay in ethanol and methanol.<sup>16</sup> At room temperature, the results are also conflicting. Wang et al. gave evidence for a charge-transfer kinetics governed by an exponential law,<sup>7</sup> but multiexponential decays were reported by Huppert et al. for alcohols.<sup>6</sup> Regarding these results, the presence of an activation barrier for the TICT state formation in DMABN has been

disputed.<sup>9-11,13,14,16</sup> Our experimental data show that, at room temperature, the LE state population decay, and thus the rise of the CT state population, is exponential. This indicates an activated barrier process as initially suggested by Grabowski et al.<sup>3,4</sup>

**4.2. Solvent Polarity and Substituent Effects on the Height of the Reaction Barrier.** (a) *Solvent Polarity Effect.* Tables 2, 3, 6, and 7 show a decrease of the charge-transfer time—or an increase of the charge-transfer rate—when the solvent polarity is increased, for both OMAP and DMABN except for the latter in ethylene glycol (Table 7). The increase of the TICT state formation rate in DMABN, in solvents of increasing polarity, was previously observed and interpreted as the decrease of the height of the LE → CT reaction barrier.<sup>13,14</sup> resulting from the energy stabilization of the CT state when the solvent polarity increases. From Rehm and Weller's equation,<sup>37</sup> and as previously suggested for DMABN,<sup>4</sup> the free energy change for the LE → CT reaction can be written as

$$\Delta G = E_{ox}(D) - E_{red}(A) - E_{LE} + C + E_{solv} \quad (8)$$

where  $E_{ox}(D)$  is the oxidation potential of the donor,  $E_{red}(A)$  the reduction potential of the acceptor,  $E_{LE}$  the energy of the locally excited state,  $C$  the energy due to the Coulombic energy of the radical pair formed, and  $E_{solv}$  the stabilization energy of the CT state due to solvation. The solvation energy is expected to increase with the solvent polarity and the CT state dipole moment. In Tables 2 and 3 are given for each aprotic solvent the reaction free energies  $\Delta G$  estimated from the corrected preexponential factors  $b_1$  and  $b_2$ , since in all cases a rapid equilibrium between the LE and CT states is obtained and

$$\Delta G = -RT \ln(k_1/k_2) = -RT \ln(b_1/b_2) \quad (9)$$

It is indeed seen that  $|\Delta G|$  increases when the solvent polarity increases; furthermore, it is larger for OMAP than for DMABN in polar solvents. This difference is likely to be due to these compounds having different electron donor and acceptor groups. On the other hand, the CT state of OMAP was estimated to have a permanent dipole moment of about 20 D,<sup>30,31</sup> which is larger than the values of 12–17 D reported for the TICT state of DMABN.<sup>19,38,39</sup> A larger stabilization of the CT state is thus expected for OMAP in polar solvents. In both cases, the charge-transfer rate is found to increase with the solvent polarity, giving support to previous assumptions that the barrier height is decreasing when  $|\Delta G|$  increases.<sup>13,14</sup> Since in polar solvents (except in propanol) the charge transfer is found to be faster in OMAP than in DMABN, one may conclude that the reaction barrier is lower in OMAP (provided there are no complications from, for example, solvent dynamics effects).

(b) *Substituents Effect.* Table 4 shows that the charge transfer rate decreases when the number of dimethylamino substituents increases, from OMAP to OTAP. In transient absorption experiments on OMAP solutions, we previously observed the delayed rise of an absorption band similar to that of the dimethylaniline cation radical,<sup>29-31</sup> evidencing that the substituted phenyl (dimethylanilino group, Figure 2) acts as the electron donor in the charge-transfer process in OMAP. The remaining diphenylphosphine oxide part can thus be considered as the electron acceptor, and substitution with further dimethylamino groups, from OMAP to OTAP, is expected to decrease its acceptor character. From eq 8 it is seen that, as long as the solvent is not changed, the decrease of the electron acceptor character of the acceptor group or decrease of  $E_{red}(A)$ , from OMAP to OTAP, will lead to the decrease of  $|\Delta G|$  and thus to the rise in energy of the CT state. The free energy change  $\Delta G$

estimated from the data given in Table 4 indicates that in tetrahydrofuran the CT state of OTAP is raised by about 1 kcal/mol above that of OMAP. A very rough estimation of the barrier height in this solvent can be made from the value of  $k_1$  given in the table, assuming a preexponential factor of about  $10^{12}$ – $10^{13}$  s $^{-1}$  for this rate constant. Values of about 2.15, 2.5, and 2.75 kcal/mol are, respectively, obtained for OMAP, ODAP, and OTAP. An increase of the barrier height is thus found to accompany the rise in energy of the CT state. Furthermore, the observation of an increase of the charge-transfer rate in the three derivatives in acetonitrile (section 3.2.a) confirms that the barrier height decreases when the solvent polarity increases.

**4.3. Charge Transfer and Internal Twisting.** (a) *Charge-Transfer Kinetics and Solvent Dynamics.* The trend observed for both OMAP and DMABN in protic solvents is that the charge-transfer time is shorter than the average solvation time whereas in fluid aprotic solvents the reaction time is longer than the solvation time. Many experimental and theoretical studies of intramolecular electron-transfer focused on the role of the solvent dynamics in the reaction kinetics (for example, see references in refs 40–42). Theoretical models describing the solvent as a dielectric continuum lead to the conclusion that the upper limit of the electron-transfer rate is close to the reciprocal of the longitudinal relaxation time  $\tau_L$ ,<sup>43,44</sup> although in the case of activated electron-transfer reactions in non-Debye solvents, the role of short-time-range solvent dynamics was stressed.<sup>45</sup> Experimental data reported by Huppert et al. showed that the electron-transfer kinetics can be correlated to  $\tau_L$ .<sup>46</sup> A solvent-controlled charge transfer was proposed for bianthryl where the charge-transfer kinetics was found to follow the solvation dynamics  $\tau_s$ ,<sup>47</sup> although a recent study contradicts this proposal and proposes instead that in this molecule the charge-transfer process involves an intramolecular torsional mode.<sup>48</sup>

For OMAP, the observation of a charge-transfer rate faster than solvation dynamics is in contradiction with the results reported by Hara et al.<sup>49,50</sup> As a matter of fact, these authors reported a triexponential decay for the LE state of this compound with an average initial decay time longer than the solvation time. However, they did not take into account the possible coexistence of oxidized and nonoxidized forms of the triphenylphosphine derivative in freshly prepared solutions. We recently showed that one component of the multiexponential fluorescence decays is due to the nonoxidized substituted triphenylphosphine.<sup>31,32</sup>

Charge-transfer kinetics faster than solvation dynamics were previously reported by Su and Simon for DMABN at low temperature,<sup>16</sup> for which nonexponential time kinetics are uniformly observed in the linear alcohols beyond ethanol. These authors analyzed their data with the Sumi–Nadler–Marcus approach,<sup>51,52</sup> which assumes that not only the solvent diffusive motion contributes to the charge-transfer process but also a vibrational mode of the solute. Considering the solvent as a dielectric continuum, this model predicts that an electron transfer involving an intramolecular mode can occur in a time range shorter than the longitudinal relaxation time  $\tau_L$  with an average transfer time that depends on  $\tau_L$  in a power law form,  $\tau_{CT} \propto \tau_L^\alpha$  ( $0 < \alpha \leq 1$ ). Su and Simon found that the average charge-transfer time in DMABN, in a series of linear alcohols between  $-50$  and  $0$  °C, was faster than the collective hydrogen-bond motions  $\tau_L$  of these alcohols and obtained  $\alpha = 0.5$ . They concluded that the reaction rate is determined by intramolecular motions and not by solvent diffusion.<sup>16</sup>

Two-dimensional theoretical approaches were recently developed to calculate the TICT state formation rate in DMABN by Fonseca et al.,<sup>21,22</sup> Polimeno et al.,<sup>23</sup> and Kim and Hynes,<sup>24</sup> where the torsional motion of the dimethylamino group is

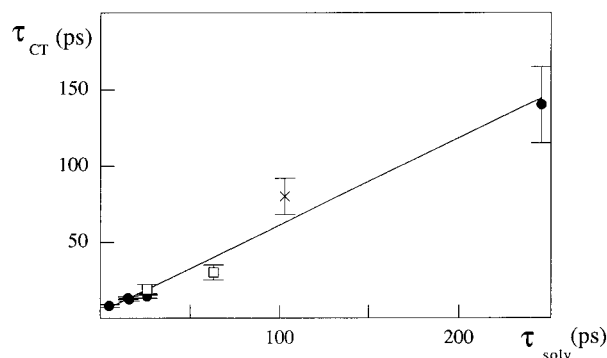


**Figure 10.** Charge-transfer time found for DMABN in a few protic solvents as a function of the average solvation time of these solvents: (●) data obtained in the present study (Table 7) (the solvation time of 1-propanol was used for 2-propanol); (□) data in 1-propanol and in butanol from Wang et al.;<sup>7,8</sup> (×) data in 1-pentanol from Okada et al.,<sup>15,25</sup> although the contribution of an extra short component of about 10 ps was considered.

considered in addition to the solvent motion. In Kim and Hynes' model,<sup>24</sup> solvent dissipative frictional damping is included on both the intramolecular and solvent coordinates and both the inertial and dissipative solvation dynamics are included in the friction on the solvent coordinate. The model predicts a solvent-dependent reaction route on the two-dimension excited-state free energy surface. The reaction coordinate for the barrier crossing can be predominantly either the intramolecular motion or the solvent motion depending on the relative magnitude of the intramolecular motion frequency and that of the inertial solvent motion. In methanol the barrier crossing is found to be mainly on the solvent coordinate whereas in acetonitrile it is mainly on the twisting motion.<sup>21,22,24</sup> Furthermore, the model predicts the solvent polarity effect on the barrier height discussed in section 4.2. The calculated charge-transfer times for DMABN in acetonitrile, methanol and ethanol with this model<sup>24</sup> are respectively 6.5, 8.1, and 11.0 ps, in good agreement with the present experimental data (Tables 3 and 7). This agreement gives confidence in the mechanism initially proposed to explain the excited-state properties of this molecule.<sup>1–4</sup>

Surprisingly, it is worth noting in Figure 10 that although an intramolecular mode is involved in the charge-transfer process, the charge-transfer time in DMABN in protic solvents is found to increase linearly with the average solvation time. The figure includes data from Wang et al. in 1-propanol<sup>7</sup> and in butanol<sup>8</sup> as well as Okada et al. in 1-pentanol,<sup>15,25</sup> although in the latter case an extra short component was invoked. Since in these solvents the charge-transfer time is less than the solvation time, the standard theories of activated charge transfer (with exponential time kinetics) that predict a proportionality between the two cannot be valid (see for example ref 43). On the other hand, although the Kim and Hynes' calculations<sup>24</sup> for two of these protic solvents (methanol and ethanol) agree well with the experimental data reported in the present study, it was shown within the model that the solvation dynamics was not involved in determining the charge transfer rate. Therefore further experimental and theoretical studies, in alcohols of long solvation times at room temperature, would be especially interesting to try to understand the meaning of this apparent correlation.

The similarity between the results observed for OMAP and DMABN suggests that the charge-transfer process involves also an intramolecular motion in OMAP. In a previous study, Vogel et al.<sup>28</sup> suggested that the dual fluorescence of polar solutions of dimethylamino-substituted triphenylphosphines is due to the formation of a TICT-like state involving the rotational motion

of the whole substituted anilino group. In transient absorption experiments we found<sup>29–31</sup> that the absorption spectrum of the charge transfer state is very similar to that of the dimethylaniline cation radical, which proves that in OMAP the charge transfer does not imply the twist of the dimethylamino group. The intramolecular mode involved in the charge transfer in OMAP is thus different from that in DMABN.

(b) *Solvent Viscosity Effect and Intramolecular Twisting Mode.* The solvent viscosity effect on the TICT state formation process in DMABN has been previously considered in several studies. The apparent viscosity effect on the LE state decay was explained either by a true viscosity dependence<sup>5,17,18,53,54</sup> or by a hidden polarity effect.<sup>14</sup> When the temperature was lowered at constant viscosity, it was shown that the charge-transfer rate increases due to the increase of the solvent polarity, which leads to the decrease of the barrier height.<sup>14</sup> We indeed noted in the present study the increase of the charge-transfer rate when the solvent polarity increases, in both protic and fluid aprotic solvents.

Since triacetin and tetrahydrofuran have nearly the same dielectric constant, true solvent viscosity effects might be observed in comparing the charge-transfer time in these solvents (Tables 2 and 3). Viscosity effect is observed only for OMAP. We suggest that the difference between OMAP and DMABN is due to the fact the charge-transfer reaction in these compounds involves a different intramolecular coordinate. Grote and Hynes' theory<sup>55</sup> predicts that the barrier crossing rate in an activated process in solution is determined by the events that occur in the solvent on the time scale of the order of the reciprocal of the barrier frequency. Thus this theory predicts viscosity effects (that is, long-time range hydrodynamic friction effects<sup>56,57</sup>) on low-frequency barriers. When the solvent is changed from tetrahydrofuran to triacetin, the decrease in the charge-transfer rate observed for OMAP and not for DMABN may thus indicate a lower barrier frequency for the reaction in OMAP, which is compatible with the lower barrier height (rounder) found for this compound. This might also be correlated to a lower intramolecular torsional frequency. Indeed, the reaction barrier frequency in DMABN ( $\omega_b = 18 \text{ ps}^{-1}$ ) was found<sup>24</sup> to be close to that of the dimethylamino torsional frequency ( $\omega_R = 15 \text{ ps}^{-1}$ ). The fact that the charge-transfer rate in OMAP is further slowed down in the protic solvent decanol, which has the same polarity but is less viscous than triacetin, might indicate that the coordinate involved in the barrier crossing is different in this solvent and thus that the friction opposed to the reaction has a different origin. Kim and Hynes demonstrated that the solvent hydrodynamic friction in fictitious viscous acetonitrile, methanol, and ethanol does not play a significant role in the barrier crossing in DMABN and consequently that no viscosity effect is expected for this compound,<sup>24</sup> in agreement with our present observations although the results in decanol remain to be explained. We are very tempted to conclude that the viscosity effect on the charge-transfer kinetics in OMAP, when comparing tetrahydrofuran and triacetin, is a good indication that the charge-transfer process involves the rotational motion of the whole anilino group since this motion is likely to occur at lower frequency than the torsion of the dimethylamino group in DMABN.

## 5. Conclusion

The kinetics of the photoinduced intramolecular charge transfer process that occurs in dimethylamino derivatives of the triphenylphosphine oxide in polar solvents were studied at room temperature, by time-resolved fluorescence spectroscopy with a streak camera and a UV subpicosecond excitation source.

Measurements were also carried out with solutions of the model compound (dimethylamino)benzonitrile, DMABN, under the same conditions. The charge-transfer process was found to occur within a few picoseconds to a few tens of picoseconds in both compounds depending on the solvent and, for the phosphine compounds, on the number of dimethylamino substituents. The charge-transfer rate was found to increase with the solvent polarity in a series of aprotic and protic solvents. An activated barrier charge-transfer process with a polarity-dependent barrier height is proposed to describe the kinetics, with a lower barrier in the (dimethylaminophenyl)diphenylphosphine oxide (OMAP) than in DMABN. In protic solvents, the charge-transfer time was found to be shorter than the average solvation time, except for DMABN in methanol. This result was interpreted as an indication that the charge-transfer process involves an intramolecular coordinate in addition to the solvent coordinate. The charge-transfer process in DMABN was initially suggested to involve a 90° twisting motion of the dimethylamino group.<sup>1–3</sup> The good agreement between the charge transfer times found in the present study and those recently calculated by Kim and Hynes<sup>24</sup> in a two-dimensional model gives confidence in the proposed mechanism. On the other hand, the fact that the charge-transfer process in OMAP is slowed in a viscous aprotic solvent whereas in DMABN it is not is taken as support for Rettig et al.'s initial proposal<sup>28</sup> that the rotation of the whole dimethylanilino group is involved in the charge-transfer process in this compound, in addition to the observation that its charge-transfer state absorption<sup>30,31</sup> is similar to that of the dimethylaniline cation radical.

**Acknowledgment.** This work was supported in part by the Chemistry Department of CNRS-France (GDR 1017). The authors thank Professor W. Rettig, Humboldt University, for his stimulation in the study of the triphenylphosphine derivatives. They also thank Professor J. T. Hynes, University of Colorado, for very helpful discussions during his stay in France at Saclay (CNRS, URA 331) and for useful comments on the present paper.

## References and Notes

- (1) Rotkiewicz, K.; Grellmann, K. H.; Grabowski, Z. *Chem. Phys. Lett.* **1973**, *19*, 315.
- (2) Grabowski, Z. R.; Rotkiewicz, K.; Rubaszewka, W.; Kirkor-Kaminska, E. *Acta Phys. Pol. A* **1978**, *54*, 767.
- (3) Grabowski, Z. R.; Rotkiewicz, K.; Siemiarczuk, A.; Cowley, D. J.; Baumann, W. *Nouv. J. Chim.* **1979**, *3*, 443.
- (4) Grabowski, Z. R.; Dobkowski, J. *Pure Appl. Chem.* **1983**, *55*, 245.
- (5) Rettig, W. *J. Lumin.* **1980**, *26*, 21.
- (6) Huppert, D.; Rand, S. D.; Rentzepis, P. M.; Barbara, P. F.; Struve, W. S.; Grabowski, Z. R. *J. Chem. Phys.* **1981**, *75*, 5714.
- (7) Wang, Y.; McAuliffe, M.; Novak, F.; Eisenthal, K. B. *J. Phys. Chem.* **1981**, *85*, 3736.
- (8) Wang, Y.; Eisenthal, K. B. *J. Chem. Phys.* **1982**, *77*, 6076.
- (9) Heisel, F.; Miehé, J. A. *Chem. Phys. Lett.* **1983**, *100*, 183.
- (10) Heisel, F.; Miehé, J. A. *Chem. Phys.* **1985**, *98*, 233.
- (11) Heisel, F.; Miehé, J. A.; Martinho, J. M. G. *Chem. Phys.* **1985**, *98*, 243.
- (12) Heisel, F.; Miehé, J. A. *Chem. Phys. Lett.* **1986**, *128*, 323.
- (13) Hicks, J.; Vandersall, M.; Babarogic, Z.; Eisenthal, K. *Chem. Phys. Lett.* **1985**, *116*, 18.
- (14) Hicks, J. M.; Vandersall, M. T.; Sitzmann, E. V.; Eisenthal, K. B. *Chem. Phys. Lett.* **1987**, *135*, 413.
- (15) Okada, T.; Mataga, N.; Baumann, W. *J. Phys. Chem.* **1987**, *91*, 760.
- (16) Su, S.-G.; Simon, J. D. *J. Chem. Phys.* **1988**, *89*, 908.
- (17) Hara, K.; Suzuki, H.; Rettig, W. *Chem. Phys. Lett.* **1988**, *145*, 269.
- (18) Hara, K.; Rettig, W. *J. Phys. Chem.* **1992**, *96*, 8307.
- (19) Schuddeboom, W.; Jonker, S. A.; Warman, J. M.; Leinhos, U.; Kühnle, W.; Zachariasse, K. A. *J. Phys. Chem.* **1992**, *96*, 10809.
- (20) Haar, T.; Hebecker, A.; Il'ichev, Y.; Kühnle, W.; Zachariasse, K. A. In *Fast elementary processes in chemical and biological systems*; Tramer, A., Ed.; AIP Press: Woodbury, NY, 1996; Vol. 364; p 295.



- (21) Fonseca, T.; Kim, H. J.; Hynes, J. T. *J. Mol. Liq.* **1994**, *60*, 161.
- (22) Fonseca, T.; Kim, H. J.; Hynes, J. T. *J. Photochem. Photobiol. A* **1994**, *82*, 67.
- (23) Polimeno, A.; Barbon, A.; Nordio, P. L.; Rettig, W. *J. Phys. Chem.* **1994**, *98*, 12158.
- (24) Kim, H.; Hynes, J. T. *J. Photochem. Photobiol. A* **1997**, *105*, 337–343.
- (25) Okada, T. In *Experimental and theoretical aspects of excited-state electron transfer and related phenomena*; Pultusk: Poland, 1992; Poster 46.
- (26) Rettig, W. *Angew. Chem., Int. Ed. Engl.* **1986**, *25*, 971.
- (27) Bonacic-Koutecky, V.; Heisel, F.; Lippert, E.; Miehe, J. A.; Rettig, W. *Adv. Chem. Phys.* **1987**, *68*, 1.
- (28) Vogel, M.; Rettig, W.; Heimbach, P. *J. Photochem. Photob. A* **1991**, *61*, 65.
- (29) Changenet, P.; Plaza, P.; Martin, M. M.; Meyer, Y. H.; Rettig, W. In *Fast elementary processes in chemical and biological systems*; Tramer, A., Ed.; AIP Press: Woodbury, NY, 1996; Vol. 364; p 363.
- (30) Changenet, P.; Plaza, P.; Martin, M. M.; Meyer, Y. H.; Rettig, W. *J. Chim. Phys.* **1996**, *93*, 1697.
- (31) Changenet, P. Thesis, Université Paris-sud, Orsay, France, 1996.
- (32) Changenet, P.; Plaza, P.; Martin, M. M.; Meyer, Y. H.; Rettig, W. *Chem. Phys.* **1997**, *221*, 311.
- (33) Beens, H.; Knibbe, H.; Weller, A. *J. Chem. Phys.* **1967**, *47*, 1183.
- (34) Dai Hung, N.; Plaza, P.; Martin, M. M.; Meyer, Y. H. *Appl. Opt.* **1992**, *31*, 7046.
- (35) Goetz, H.; Nerdel, F.; Wiechel, K.-H. *J. L. Ann. Chem.* **1963**, *665*, 1.
- (36) Horng, M. L.; Gardecki, J. A.; Papazyan, A.; Maroncelli, M. *J. Phys. Chem.* **1995**, *99*, 17311.
- (37) Rehm, D.; Weller, A. *Isr. J. Chem.* **1970**, *8*, 259.
- (38) Rettig, W. *J. Mol. Struct.* **1982**, *84*, 303.
- (39) Baumann, W.; Bischof, H.; Fröling, J.-C.; Brittinger, C.; Rettig, W.; Rotkiewicz, K. *J. Photochem. Photobiol. A* **1992**, *64*, 49.
- (40) Weaver, M. J.; McManis III, G. E. *Acc. Chem. Res.* **1990**, *23*, 294.
- (41) Barbara, P. F.; Walker, G. C.; Smith, T. P. *Science* **1992**, *256*, 975.
- (42) Yoshihara, K. In *Ultrafast processes in chemistry and photobiology*; El-Sayed, Tanaka, I., Molin, Y., Eds.; Blackwell Science: Oxford, 1995; p 105.
- (43) Zusman, L. D. *Chem. Phys.* **1980**, *49*, 295.
- (44) Rips, I.; Jortner, J. *J. Chem. Phys.* **1987**, *87*, 2090.
- (45) Hynes, J. T. *J. Phys. Chem.* **1986**, *90*, 3701.
- (46) Huppert, D.; Kanety, H.; Kosower, E. M. *Faraday Discuss.* **1982**, *74*, 1.
- (47) Kang, T. J.; Jarzaba, W.; Barbara, P. F.; Fonseca, T. *Chem. Phys.* **1990**, *149*, 81.
- (48) Mataga, N.; Nishikawa, S.; Okada, T. *Chem. Phys. Lett.* **1996**, *257*, 327.
- (49) Hara, K.; Kometani, N.; Kajimoto, O. *Chem. Phys. Lett.* **1994**, *225*, 381.
- (50) Hara, K.; Kometani, N.; Kajimoto, O. *J. Phys. Chem.* **1996**, *100*, 1488.
- (51) Sumi, H.; Marcus, R. A. *J. Chem. Phys.* **1986**, *84*, 4894.
- (52) Nadler, W.; Marcus, R. A. *J. Chem. Phys.* **1987**, *86*, 3906.
- (53) Braun, D.; Rettig, W. *Chem. Phys.* **1994**, *180*, 231.
- (54) Rettig, W. *J. Phys. Chem.* **1982**, *86*, 1970.
- (55) Grote, R. F.; Hynes, J. T. *J. Chem. Phys.* **1980**, *76*, 2715.
- (56) Levesque, D.; Verlet, L. *Phys. Rev. A* **1970**, *2*, 2514.
- (57) Grote, R. F.; Zwan, G. v. d.; Hynes, J. T. *J. Phys. Chem.* **1984**, *88*, 4676.
- (58) Riddick, J. A.; Bunger, W. B. *Organic Solvents*, 3rd ed.; Wiley-Interscience: New York, 1970; Vol. II.
- (59) Kahlow, M. K.; Kang, T. J.; Barbara, P. F. *J. Chem. Phys.* **1988**, *88*, 2372.
- (60) Chang, Y. J.; Castner, E. W. *J. Chem. Phys.* **1993**, *99*, 7289.
- (61) Walker, G. C.; Akesson, E.; Johnson, A. E.; Levinger, N. E.; Barbara, P. F. *J. Phys. Chem.* **1992**, *96*, 3728.
- (62) Ben-Amotz, D.; Harris, C. B. *J. Chem. Phys.* **1987**, *86*, 4856.